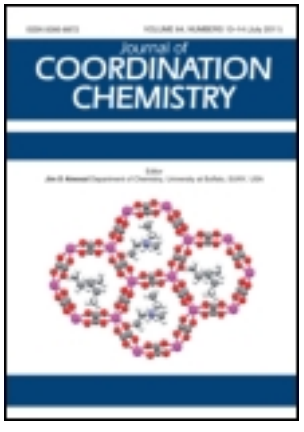

Journal of Coordination Chemistry
Publication details, including instructions for authors and subscription information:
http://www.tandfonline.com/loi/gcoo20

Electrochemical investigation and DNA-binding studies of pefloxacin-metal(II/III) complexes

Harun Muslu [a], Aysegul Golcu [a], Mehmet Tumer [a] & Mehmet Ozsoz [b]

[a] Department of Chemistry, Faculty of Science and Letters, University of Kahramanmaras Sutcu Imam, Campus of Avsar 46100, Kahramanmaras, Turkey

[b] Department of Analytical Chemistry, Faculty of Pharmacy, Ege University, 35100 Izmir, Turkey

Published online: 21 Oct 2011.

To cite this article: Harun Muslu, Aysegul Golcu, Mehmet Tumer & Mehmet Ozsoz (2011) Electrochemical investigation and DNA-binding studies of pefloxacin-metal(II/III) complexes, Journal of Coordination Chemistry, 64:19, 3393-3407, DOI: 10.1080/00958972.2011.610103

To link to this article: http://dx.doi.org/10.1080/00958972.2011.610103

Journal of Coordination Chemistry
Vol. 64, No. 19, 10 October 2011, 3393–3407

Electrochemical investigation and DNA-binding studies of pefloxacin–metal(II/III) complexes

HARUN MUSLU†, AYSEGUL GOLCU*†, MEHMET TUMER† and MEHMET OZSOZ‡

†Department of Chemistry, Faculty of Science and Letters, University of Kahramanmaras Sutcu Imam, Campus of Avsar 46100, Kahramanmaras, Turkey
‡Department of Analytical Chemistry, Faculty of Pharmacy, Ege University, 35100 Izmir, Turkey

(*Received 13 May 2011; in final form 15 July 2011*)

Complexes of pefloxacin (PEF), with Cu(II), Zn(II), Pt(II), Ru(III), and Fe(III) have been synthesized and characterized by spectroscopic techniques involving UV-Vis, IR, ^{1}H-HMR, CHN elemental analysis, electrochemical, and thermal behaviors. The electrochemical properties of all complexes were investigated by cyclic voltammetry (CV) using a glassy carbon electrode. The biological activities of the complexes have been evaluated by examining their ability to bind to calf thymus DNA (CT-DNA) with UV spectroscopy and CV. UV studies of the interaction of the complexes with DNA show that these compounds can bind to CT-DNA and the binding constants have been calculated. The cyclic voltammograms of the complexes in the presence of CT-DNA show that the complexes can bind to CT-DNA by intercalative and electrostatic binding. The antimicrobial activities of these complexes have been evaluated against three Gram-positive and four Gram-negative bacteria. Antifungal activities against two different fungi have been evaluated and compared with pefloxacin as reference. Almost all complexes show excellent activity against all bacteria and fungi.

Keywords: Drug–metal complex; Pefloxacin; DNA binding; Voltammetry

1. Introduction

Drugs are typically polyfunctional compounds, designed to interact with specific receptors or organs. Quinolone family drugs are frequently used to treat various bacterial infections because of their broad spectrum antibacterial activities [1]. Pefloxacin (1-ethyl-6-fluoro-7-(4-methylpiperazin-1-yl)-4-oxo-quinoline-3-carboxylic acid) (scheme 1), is a member of second generation fluoroquinolone antibiotics, with high activity against both Gram-positive and Gram-negative bacteria, and also show significant activity against anaerobic bacteria [2]. Quinolones comprise a group of well-known antibacterial agents with the first members being in clinical practice over 40 years [3, 4]. PEF inhibits the enzyme DNA gyrase in bacteria which is responsible for super coiling of DNA [5]. They act as antibacterial drugs that effectively inhibit DNA

*Corresponding author. Email: ag518@ksu.edu.tr

ISSN 0095-8972 print/ISSN 1029-0389 online © 2011 Taylor & Francis
http://dx.doi.org/10.1080/00958972.2011.610103

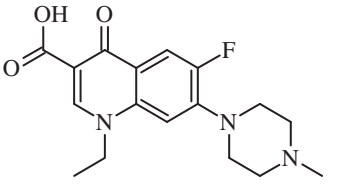

Scheme 1. 1-Ethyl-6-fluoro-7-(4-methylpiperazin-1-yl)-4-oxo-quinoline-3-carboxylic acid (pefloxacin).

replication and are commonly used in treatment of many infections [6, 7]. Recent research has shown that in the presence of divalent cations, antimicrobial effects of fluoroquinolones are changed. Fluoroquinolones also affect trace metal metabolism by inhibiting copper- and zinc-dependent enzymes [1]. Fluoroquinolones play an important biological role by chelating with certain metal ions with the carbonyl and the carboxyl group of the molecule [2].

The antibacterial activity under identical experimental conditions formed a straight relationship with the uptake data [3]. Drug permeation into cells related to its net charge was suggested. The molecule in zwitterionic form shows maximum permeation properties while the uptake was diminished when the drug bears a net charge as a result of ionization or complex formation with divalent ions [4].

A variety of functional groups originate reactivity toward metal cations. The design of metal–drug complexes are of particular interest in pharmacological research. Metal combinations with pharmaceutical agents improve drug activity, to decrease their toxicity and gain an ability to act as regulator for gene expression and a tool for microbiology [6]. Quinolone antibiotics are chelating agents for a variety of metal ions and well-known for their biological activity [7–10]. There is a difficulty in synthesizing quinolone metal complexes, because of low solubility of quinolones and their metal complexes in the pH range 5–10. In recent years, the structure, the spectroscopic and the biological properties of diverse metal complexes with various quinolone antibacterial drugs have been studied [11–17].

Interactions of transition-metal complexes with DNA have been an active field of research. Interest stems from attempts to gain some insight into the interaction between DNA and complexes, and obtain some information about drug design and tools of molecular biology [18–20]. Transition metal complexes can interact with DNA through electrostatic interaction, groove binding, and intercalation. Binding to DNA through intercalation with planar ligands intercalating into the adjacent base pairs of DNA [20] correlates with the planarity of the ligand, coordination geometry of the metal ion, and donor type of the ligand [21]. Applications of these complexes to develop complexes with fully planar structures intercalating into the adjacent base pairs of DNA [22] give valuable information to explore potential chemotherapeutical agents. Many metal complexes, which possess biologically accessible redox potentials and demonstrate high nucleobase affinity, have been synthesized and their interactions with DNA have been studied [23–30].

Electrochemical investigations of nucleic acid binding molecules–DNA interactions can provide a useful complement to spectroscopic techniques, yield information about the mechanism of intercalation, and confirm anti HIV–DNA adduct. Immobilization of DNA on an electrode surface is crucial to developing DNA biosensors for monitoring

drugs or complexes because it dictates the accessibility of the DNA to drugs or complexes in solution and hence can influence the affinity of drug binding. Binding of drugs or complexes to DNA and general DNA damage has been described through variation of the electrochemical signal of guanine [31, 32] or adenine [33, 34]. Observing the electrochemical signal related to DNA–drug or DNA–complex interaction can provide evidence for interaction mechanism and the nature of the complex formed, binding constant, size of binding site, and the role of free radicals generated during interaction in drug or complex action. A good sensitivity of oxidation signals for DNA structure would make carbon electrodes useful in DNA research, especially pencil graphite electrode [34], Pt electrode [20], and glassy carbon electrode (GCE) [35, 36].

The aim of this study was explaining the coordination behavior of PEF toward some transition metals using different tools of analysis. Thermal and electrochemical behaviors of PEF and its metal complexes were investigated in detail and different electrochemical parameters were calculated. The complex has been tested for its ability to bind to calf thymus (CT) DNA. The binding properties of the complex with CT-DNA have been investigated with UV and cyclic voltammetry (CV) titrations. Antibacterial and antifungal properties of PEF and complexes were studied against both Gram-positive and Gram-negative bacteria.

2. Experimental

2.1. *Materials and reagents*

Pefloxacin was kindly provided by Eczacibaşi Drug Comp. (Istanbul, TURKEY) while solvents and chemicals of analytical grade were purchased. Metal salts ($CuCl_2{\cdot}2H_2O$, $ZnCl_2$, $FeCl_3{\cdot}6H_2O$, K_2PtCl_4, and $RuCl_2{\cdot}3H_2O$), NaCl, and Tris-HCl were purchased from Merck. CT-DNA was purchased from Sigma. DNA stock solution was prepared by dilution of CT-DNA to buffer solution (containing 150 mmol L^{-1} NaCl and 15 mmol L^{-1} Tris-HCl at pH 7.0) followed by exhaustive stirring at 4°C for 3 days [20], and kept at 4°C for no longer than a week. The stock solution of CT-DNA gave a ratio of UV absorbance at 260 and 280 nm (A_{260}/A_{280}) of 1.89, indicating that the DNA was sufficiently free of protein contamination [37]. The DNA concentration was determined by the UV absorbance at 260 nm after 1 : 20 dilution using $e = 6600$ $(\text{mol L}^{-1})^{-1}\text{cm}^{-1}$ [38, 39].

2.2. *Instruments*

Elemental analyses (C, H, N) were performed using an LECO CHNS 932 elemental analyzer. IR spectra were obtained using an ATR component (4000–30 cm^{-1}) on a Perkin Elmer LX-125000B FT-IR spectrophotometer. Electronic spectra from 200 to 900 nm were obtained on a Perkin Elmer Lambda 45 spectrophotometer. Thermal analyses of the complexes were performed on a Perkin Elmer Pyris Diamond DTA/TG Thermal System under nitrogen at a heating rate of 10°C min^{-1}. ^{1}H-NMR spectra of the compounds were performed on a Bruker Avance DPX-400 in DMSO. Molar conductances of the metal complexes were determined in DMF ($\sim 10^{-3}$ mol L^{-1}) at room temperature using a Jenway Model 4070 conductivity meter. Mass spectra of the

ligands were recorded on an LC/MS APCI AGILENT 1100 MSD spectrophotometer. Magnetic measurements were carried out by the Gouy method using Hg[Co(SCN)] as calibrant.

All voltammetric measurements at the GCE were performed using a BAS 100W (Bioanalytical System, USA) electrochemical analyzer. A glassy carbon working electrode (BAS; Φ: 3 mm diameter), an Ag/AgCl reference electrode (BAS; 3 mol L^{-1} KCl), platinum wire counter electrode, and a standard one-compartment three electrode cell of 10 mL capacity were used in all experiments. The GCE was polished manually with aqueous slurry of alumina powder (Φ: 0.01 cm) on a damp smooth polishing cloth (BAS velvet polishing pad) before each measurement. All measurements were at room temperature. A Mettler Toledo MP 220 pH meter was used for pH measurements using a combined electrode (glass electrode reference electrode) with an accuracy of ±0.05 pH.

2.3. *Synthesis of the metal complexes*

2.3.1. Synthesis of copper(II) complex. Copper(II) complex (scheme 2) was obtained according to a general procedure: A solution of a metal salt (1 mmol, $CuCl_2 \cdot H_2O$) dissolved in 5 mL of MeOH was added to a solution of PEF (2 mmol) in 5 mL of distilled water and finally 15 mL of MeOH was added and the mixture was heated under reflux for 1 day. At the end of the reaction, determined by TLC, the precipitate was filtered off, washed with distilled water, EtOH, and dried under vacuum.

2.3.2. Synthesis of zinc(II), platinum(II), ruthenium(III), and iron(III) complexes. Zinc(II), platinum(II), iron(III), and ruthenium(III) complexes were obtained according to a general procedure: A solution of metal salt (1 mmol) dissolved in 5 mL of MeOH was added to a solution of PEF (1 mmol) in 5 mL of distilled water

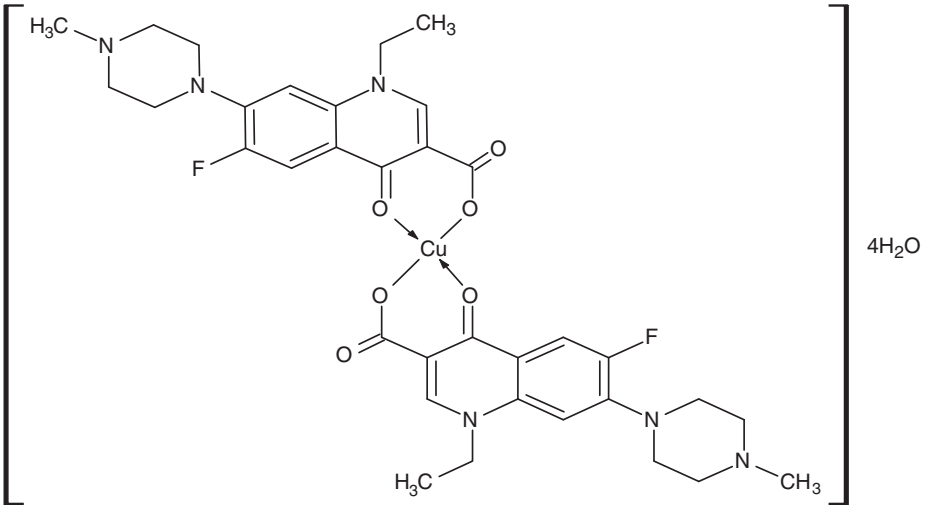

Scheme 2. Proposed structure of $[Cu(PEF)_2] \cdot 4H_2O$.

and finally 15 mL of MeOH was added and the mixture was heated under reflux for 1 day. At the end of the reaction, determined by TLC, the precipitate was filtered off, washed with distilled water, EtOH, and dried under vacuum. The proposed formulae of M(II)-PEF and M(III)-PEF complexes are given in schemes 3 and 4, respectively.

2.4. *Biological activity*

The antibacterial activities of PEF and its synthesized metal chelates were screened *in vitro* using the disc diffusion method. The chosen strains, *Candida albicans*, *Saccharomyces cerevisiae*, *Escherichia coli*, *Enterobacter cloacae*, *Bacillus megaterium*, *Bacillus cereus*, *Pseudomonas* sp., *Brucella melitensis,* and *Staphylococcus aureus*, were obtained from the Microbiology Laboratory, Department of Biology, Faculty of Science and Arts, Kahramanmaras, Turkey. Test solutions of PEF and its Cu(II), Zn(II), Pt(II), Fe(III), and Ru(III) complexes were prepared in DMSO. The bacteria were cultured for 24 h at 37°C in an incubator. Muller Hinton broth was used for preparing basal media for the bioassay of the organisms. Nutrient agar was poured onto a plate and allowed to solidify. The test solutions (DMSO) were added dropwise to a 10 mm diameter filter paper disc at the center of each agar plate. The plates were then

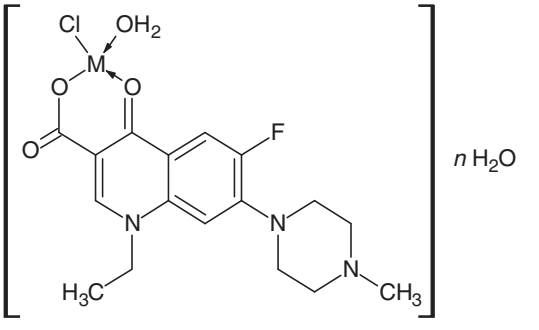

Scheme 3. Proposed structures of Zn(II) and Pt(II) complexes ($n=3$ for Pt(II) and $n=0$ for Zn(II) complexes).

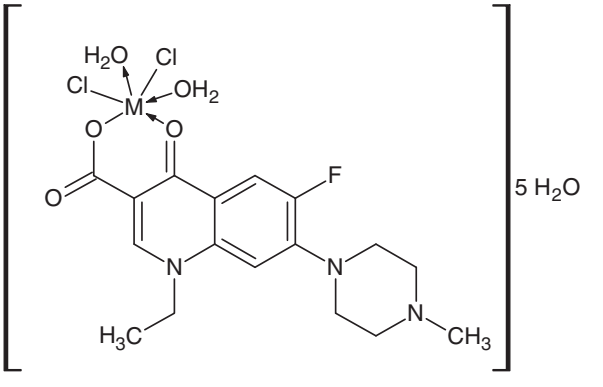

Scheme 4. Proposed structures of Ru(III) and Fe(III) complexes.

kept at 5°C for 1 h and transferred to an incubator maintained at 37°C. The width of the growth inhibition zone around the disc was measured after 24 h incubation.

3. Results and discussion

3.1. *Spectroscopic studies*

Cu(II), Zn(II), Pt(II), Fe(III), and Ru(III) complexes of PEF were synthesized using molar ratios of PEF : M = 2 : 1 for Cu(II) and 1 : 1 for Zn(II), Pt(II), Fe(III), and Ru(III). The analytical data and physical properties of the complexes are summarized in table 1. The found and calculated percentages of C, H, and N agree, confirming the suggested molecular structure. Diverse crystallization techniques were employed to obtain a crystal suitable for structure determination with X-ray crystallography. Nevertheless, the complexes were collected as microcrystalline products [40, 41].

3.1.1. IR absorption studies. IR spectra of PEF and its metal complexes are listed in table 2 and "Supplementary material". All PEF complexes show a broad band between 3335 and 3402 cm^{-1}, which corresponds to ν(O–H). The ν(C=O) of the ketone is at 1613–1627 cm^{-1}. In all spectra of the complexes, there is a new band at 550–632 cm^{-1}, corresponding to $\nu(M–OOC)_{acid}$. These bands are absent in the spectrum of PEF, showing metal coordination to carboxylic acid [42]. Also, there are new bands between 382 and 461 cm^{-1}, corresponding to ν(M–O) and between 271 and 316 cm^{-1}, related to ν(M–Cl).

Table 1. Analytical and physical properties of pefloxacin complexes.

Compound	Formula weight ($g\,mol^{-1}$)	Color	Yield (%)	Freezing point (°C)	Elemental analysis; Calcd (Found)		
					C	H	N
$[Cu(PEF)_2]\cdot 4H_2O$	800.21	Blue	80	297	51.06 (50.98)	5.714 (5.49)	9.991 (10.49)
$[Pt(PEF)Cl(H_2O)]\cdot 3H_2O$	497.62	Brown	74	307	2.54 (32.07)	3.842 (3.77)	6.018 (6.669)
$[Fe(PEF)Cl_2(H_2O)_2]\cdot 5H_2O$	502.24	Orange	86	318	38.26 (38.21)	3.61 (3.65)	8.37 (8.39)
$[Zn(PEF)Cl(H_2O)]$	497.62	White	82	298	45.25 (44.53)	4.69 (4.79)	9.31 (8.82)
$[Ru(PEF)Cl_2(H_2O)_2]\cdot 5H_2O$	764.19	Black	91	323	28.45 (28.34)	5.49 (4.15)	5.49 (5.52)

Table 2. FAR- and MID-IR results of PEF and its metal complexes.

Compound	ν(OH)	$\nu(C=O)_{ketone}$	$\nu(M–OOC)_{acid}$	ν(M–O)	ν(M–Cl)
PEF	3335	1625	–	–	–
$[Cu(PEF)_2]\cdot 4H_2O$	3402	1615	593	442	–
$[Pt(PEF)Cl(H_2O)]\cdot 3H_2O$	3376	1626	562	461	313
$[Fe(PEF)Cl_2(H_2O)_2]\cdot 5H_2O$	3388	1613	632	447	316
$[Zn(PEF)Cl(H_2O)]$	–	1627	550	450	287
$[Ru(PEF)Cl_2(H_2O)_2]\cdot 5H_2O$	3390	1627	555	382	271

Table 3. Spectroscopic data of PEF metal complexes.

Compound	π–π^* (nm)	n–π^* (nm)	Charge transfer (nm) (M → L or L → M)	d–d* (nm)
[Zn(PEF)Cl(H_2O)]	264	312	384	–
[Ru(PEF)Cl_2(H_2O)$_2$]·5H_2O	242	324	422	547
[Fe(PEF)Cl_2(H_2O)$_2$]·5H_2O	244	308	381	560
[Pt(PEF)Cl(H_2O)]·3H_2O	252	326	403	–
[Cu(PEF)$_2$]·4H_2O	245	345	428	603

3.1.2. Electronic spectra. Formation of the complexes was confirmed by UV-Vis spectra (table 3) in acetonitrile/water (1/1, v/v). All complexes except Pt(II) and Zn(II) complexes show d–d transitions between 523 and 603 nm [4]. The spectra of the complexes show bands between 381 and 428 nm assigned to M → L and L → M (L: Ligand, M: Metal) charge transfer transitions. There are $n \rightarrow \pi^*$ and $\pi \rightarrow \pi^*$ transitions between 308 and 345 nm and 242 and 264 nm, respectively.

The magnetic moments (as BM) of the complexes were measured at room temperature. The Ni(II) and Pt(II) complexes are diamagnetic and square planar around the metal. The structures of the Cu(II) complex are supported by the magnetic moment data of 1.77 BM, which is very close to that of the spin only value (1.73 BM). This value suggests tetrahedral copper [43]. The observed magnetic moment of Fe(III) is 5.27 BM. Magnetic susceptibility of the Ru(III) complex at 298 K showed an effective magnetic moment μ_{eff} of 1.90 BM.

The molar conductivity measurements were done on all compounds in DMSO ($\sim 1.10^{-3}$ mol L^{-1} solutions). The conductivity data of the complexes are very low and can be regarded as nonelectrolytes [44].

3.1.3. The ^{1}H NMR studies. The molecular structures of complexes were also examined by nuclear magnetic resonance (NMR) spectroscopy. NMR spectra of PEF showed a singlet at 2.345 ppm for protons of piperazine N-methyl, 7.271 and 7.969 ppm for aromatic protons, and finally singlet at 10.841 ppm for the proton of carboxylic acid. A doublet occurs at 3.571 for the four protons of piperazine. Comparing the main peaks of complexes with that of PEF, proton NMR spectra are almost identical to PEF except for the absence of carboxylic acid proton (Supplementary material), suggesting coordination of PEF through its carboxylate oxygen [45].

3.1.4. Thermogravimetric analysis. Thermal behaviors of the complexes were characterized using TGA and TGA/DTG (Supplementary material). The DTA/TG measurements were carried out from 25 to 1000°C. Thermal decompositions occurred in three steps. In the first step, the complexes lose water between 75 and 120°C. This is consistent with the C, H, and N elemental analyses. In the second step, chlorides are lost from 150 to 300°C. In the last step, there were large decreases in weight because of the decomposition of the organic parts to metal oxides. These results agreed with the proposed structures of the complexes [45].

3.2. *Electrochemical studies*

Cathodic determination of PEF has been studied using a hanging mercury electrode (HME) by Beltagi [46]. Anodic behavior and determination of PEF on boron-doped diamond and GCEs were investigated using cyclic, linear sweep, differential pulse, and square wave voltammetric techniques by Uslu *et al*. [47].

PEF, $[Cu(PEF)_2]\cdot 4H_2O$, $[Zn(PEF)Cl(H_2O)]$, $[Pt(PEF)Cl(H_2O)]\cdot 3H_2O$, $[Fe(PEF)Cl_2(H_2O)_2]\cdot 5H_2O$, and $[Ru(PEF)Cl_2(H_2O)_2]\cdot 5H_2O$ were subjected to a cyclic voltammetric study to characterize their electrochemical behavior on the GCE. Electrochemical behaviors were studied over a wide pH range (1.0–12.0) with a glassy carbon disc electrode in buffered aqueous media.

Cyclic voltammetric behavior of PEF and its transition metal complexes, except $[Cu(PEF)_2]\cdot 4H_2O$, yielded a well-defined peak at all pH values; $[Cu(PEF)_2]\cdot 4H_2O$ has two well-defined peaks depending on the pH for GCE (Supplementary material). The scanning was started at −0.20 V in the positive direction at pH 2.0 phosphate buffer; anodic oxidation of PEF did not occur until about 1.20 V for GCE. By reversing at high potentials no reduction wave or peak corresponding to the anodic peaks were observed on the cathodic scan for GCE. Typical cyclic voltammograms of $[Cu(PEF)_2]\cdot 4H_2O$, $[Zn(PEF)Cl(H_2O)]$, $[Pt(PEF)Cl(H_2O)]\cdot 3H_2O$, $[Ru(PEF)Cl_2(H_2O)_2]\cdot 5H_2O$, and $[Fe(PEF)Cl_2(H_2O)_2]\cdot 5H_2O$ have been given in "Supplementary material".

Comparative CV of PEF in the presence of copper(II) ions at anodic directions for: (a) blank, (b) PEF alone, and (c) $[Cu(PEF)_2]\cdot 4H_2O$ are provided in the "Supplementary material". Evidence of complex formation is established as a result of the increase in the copper(II) peak currents at −0.136 V and 1.204 V on anodic direction as for $[Cu(PEF)_2]\cdot 4H_2O$. For other complexes, peak currents have been found at 1.191 V, 1196 V, and 1.183 V for $[Zn(PEF)Cl(H_2O)]$, $[Fe(PEF)Cl_2(H_2O)_2]\cdot 5H_2O$, and $[Ru(PEF)Cl_2(H_2O)_2]\cdot 5H_2O$, respectively.

The pH of the supporting electrolyte has a significant effect on the electroreduction of the complexes at the GCE. CV of solid synthesized complexes exhibited one or two well-defined peaks and the peaks became sharper in phosphate buffer at pH 2. Plots of pH *versus* E_p and I_p have been investigated using CV techniques. The peak potential (E_p) at the redox process moved to less positive potential values by raising the pH (Supplementary material).

The plot of the peak potential *versus* pH showed one straight line between pH 2.0 and 12.0, which can be expressed by the following equations in phosphate buffer:

$$E_p\ (\text{mV}) = 1241.10 - 39.28\ \text{pH};$$
$$R^2 = 0.8528 \text{ for } [Cu(PEF)_2]\cdot 4H_2O,$$

$$E_p\ (\text{mV}) = 1260.80 - 46.28\ \text{pH};$$
$$R^2 = 0.9004 \text{ for } [Fe(PEF)Cl_2(H_2O)_2]\cdot 5H_2O,$$

$$E_p\ (\text{mV}) = 1232.30 - 40.20\ \text{pH};$$
$$R^2 = 0.9243 \text{ for } [Pt(PEF)Cl(H_2O)]\cdot 3H_2O,$$

$$E_p\ (\text{mV}) = 1235.10 - 41.61\ \text{pH};$$
$$R^2 = 0.8999 \text{ for } [Ru(PEF)Cl_2(H_2O)_2]\cdot 5H_2O,$$

$$E_p\ (\text{mV}) = 1227.50 - 40.52\ \text{pH};$$
$$R^2 = 0.9150 \text{ for } [\text{Zn(PEF)Cl}(H_2O)].$$

The effect of pH on peak current of all complexes in the range of pH 2.0–12.0 was also evaluated. The best and sharpest peak and reproducible results were obtained in pH 2.0 phosphate buffer. Therefore, this media was chosen in this study as the supporting electrolyte for the electroanalytical investigations.

Scan rate studies were carried out to investigate whether the process at the GCE was under diffusion or adsorption control. The effects of the potential scan rate between 5 and 500 mV s^{-1} on the peak current and potential of all complexes were evaluated in pH 2 phosphate buffer. The typical current–potential curve of scan rate studies of $[Fe(PEF)Cl_2(H_2O)_2]\cdot 5H_2O$ has been given in "Supplementary material". When the scan rate was varied from 5 to 500 mV s^{-1} in 1×10^{-5} mol L^{-1} complex solutions, a linear dependence of the peak current I_p (μA) upon the square root of the scan rate $v^{1/2}$ (mV s^{-1}) was found by GCE (Supplementary material), demonstrating diffusional behavior. The equations are noted below in pH 2.0 phosphate buffer ($n = 10$ in all studies).

$$I_p\ (\mu\text{A}) = 0.0342\, \nu^{1/2}(\text{mV s}^{-1}) + 1.019,$$
$$R^2 : 0.9820 \text{ for } [Cu(PEF)_2] \cdot 4H_2O,$$

$$I_p\ (\mu\text{A}) = 0.2433\, \nu^{1/2}(\text{mV s}^{-1}) + 0.5831,$$
$$R^2 : 0.9929 \text{ for } [Fe(PEF)Cl_2(H_2O)_2] \cdot 5H_2O,$$

$$I_p\ (\mu\text{A}) = 0.0282\, \nu^{1/2}(\text{mV s}^{-1}) - 0.0481,$$
$$R^2 : 0.9908 \text{ for } [Pt(PEF)Cl(H_2O)] \cdot 3H_2O,$$

$$I_p\ (\mu\text{A}) = 0.1179\, \nu^{1/2}(\text{mV s}^{-1}) + 0.8575,$$
$$R^2 : 0.9890 \text{ for } [Ru(PEF)Cl_2(H_2O)_2] \cdot 5H_2O,$$

$$I_p\ (\mu\text{A}) = 0.0461\, \nu^{1/2}(\text{mV s}^{-1}) + 0.2270,$$
$$R^2 : 0.9894 \text{ for } [Zn(PEF)Cl(H_2O)].$$

The effect of scan rate on peak current was also examined under the above conditions with a plot of logarithm of peak current *versus* logarithm of scan rate (Supplementary material) giving a straight line within the same scan rate range. These linear relationships were obtained as follows ($n = 10$ in all studies):

$$\log I_p\ (\mu\text{A}) = 0.6552 \log \nu\ (\text{mV s}^{-1})$$
$$+0.0679 (R^2: 0.9986)$$
$$\text{for } [Cu(PEF)_2] \cdot 4H_2O,$$

$$\log I_p\ (\mu\text{A}) = 0.6289 \log \nu\ (\text{mV s}^{-1})$$
$$- 1.0267 (R^2: 0.9961)$$
$$\text{for } [Fe(PEF)Cl_2(H_2O)_2] \cdot 5H_2O,$$

$$\log I_p\ (\mu A) = 0.4317 \log \nu\ (mV\,s^{-1}) - 0.5807 (R^2: 0.9902)$$
for $[Pt(PEF)Cl(H_2O)] \cdot 3H_2O$,

$$\log I_p\ (\mu A) = 0.6828 \log \nu\ (mV\,s^{-1}) - 1.1629 (R^2: 0.9812)$$
for $[Ru(PEF)Cl_2(H_2O)_2] \cdot 5H_2O$,

$$\log I_p\ (\mu A) = 0.6369 \log \nu\ (mV\,s^{-1}) - 0.9798 (R^2: 0.9901)$$
for $[Zn(PEF)Cl(H_2O)]$.

The slopes (between 0.43 and 0.68) of the relationship are close to the theoretically expected (0.5) for an ideal reaction of solution species, so in this case the process had a diffusive component [48, 49].

3.3. *DNA-binding studies*

The mutual effect of the complexes with CT-DNA has been studied with UV spectroscopy and CV in order to investigate the possible binding modes to CT-DNA and to calculate binding constants (K_b). In UV titration experiments, the spectra of CT-DNA in the presence of each complex have been recorded for a constant CT-DNA concentration in diverse [complex]/[CT-DNA] mixing ratios (r). The intrinsic binding constants, K_b, of the complexes with CT-DNA are determined through UV spectra of the complexes recorded for a constant complex DNA concentration (4×10^{-5} mol L^{-1}) in the absence and presence of CT-DNA for diverse r values. The interaction of the complexes with CT-DNA has also been investigated by monitoring the changes observed in the cyclic voltammogram of a 1×10^{-5} mol L^{-1} (1/9 methanol/buffer solution containing) of the complexes upon addition of CT-DNA at diverse r values. Complexes are known to bind to DNA *via* both covalent and/or noncovalent interactions [39, 50]. Noncovalent DNA interactions include intercalative, electrostatic, and groove (surface) binding of metal complexes outside the DNA helix, along major or minor groove. DNA can provide three distinctive binding sites for all metal complexes, groove binding, electrostatic binding to phosphate group, and intercalation [39, 51], of importance to quinolone antibacterial in the body [52].

Figure 1 illustrates the spectral changes occurring in 1×10^{-4} mol L^{-1} methanolic solution of $[Pt(PEF)Cl(H_2O)] \cdot 3H_2O$ upon addition of increasing amounts of CT-DNA. Even though no appreciable changes in the position of the intraligand band of metal complexes are observed by the addition of CT-DNA, the intensity of the band centered at 272 nm for $[Zn(PEF)Cl(H_2O)]$ (from 272 to 261 for $[Pt(PEF)Cl(H_2O)] \cdot 3H_2O$, from 274 to 262 for $[Fe(PEF)Cl_2(H_2O)_2] \cdot 5H_2O$, and from 270 to 260 for $[Ru(PEF)Cl_2(H_2O)_2] \cdot 5H_2O$) is increased in the presence of DNA up to $r = 9$ and a blue shift of 8 nm (264 nm) is observed for higher amounts of DNA. The hypsochromic effect observed might be ascribed to external contact (electrostatic binding) [39] or that all complexes could uncoil the helix structure of DNA and make bases imbedded in

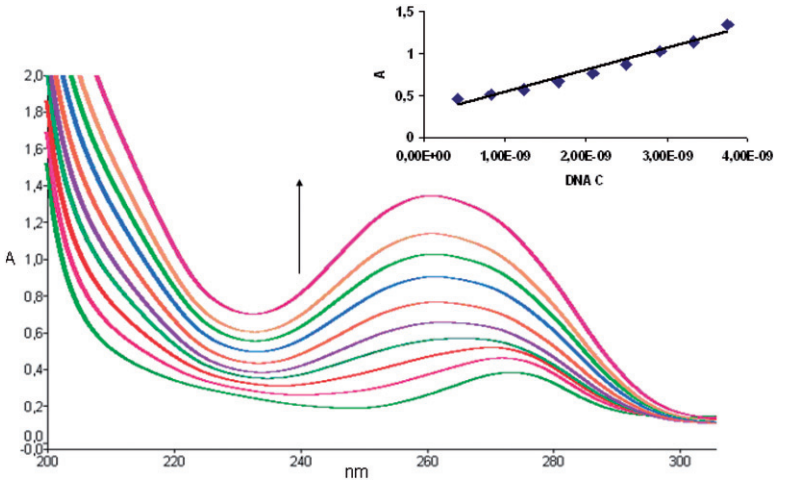

Figure 1. UV spectra of $[Pt(PEF)Cl(H_2O)]\cdot 3H_2O$ in buffer solution in the presence of CT-DNA at increasing amounts. $[Pt(PEF)Cl(H_2O)]\cdot 3H_2O = 1\times 10^{-5}\,mol\,L^{-1}$. The arrow shows that the intensity changes upon increasing concentration of CT-DNA.

Table 4. The intrinsic binding constants (K_b) of complexes with CT-DNA.

Compound	K_b (± 0.03)
$[Zn(PEF)Cl(H_2O)]$	6.67×10^7
$[Fe(PEF)Cl_2(H_2O)_2]\cdot 5H_2O$	5.00×10^7
$[Ru(PEF)Cl_2(H_2O)_2]\cdot 5H_2O$	5.00×10^7
$[Pt(PEF)Cl(H_2O)]\cdot 3H_2O$	5.00×10^8

DNA exposed [20, 40, 41, 50]. The intrinsic binding constants K_b of $[Cu(PEF)_2]\cdot 4H_2O$, $[Zn(PEF)Cl(H_2O)]$, $[Pt(PEF)Cl(H_2O)]\cdot 3H_2O$, $[Fe(PEF)Cl_2(H_2O)_2]\cdot 5H_2O$, and $[Ru(PEF)Cl_2(H_2O)_2]\cdot 5H_2O$ with CT-DNA representing the binding constant per DNA base pair, can be obtained by monitoring changes in absorbances between 274 and260 nm with increasing concentrations of CT-DNA from plots of $[DNA]/(\varepsilon_a-\varepsilon_f)$ *versus* [DNA] and is given by the ratio of slope to the y intercept, according to the following equation [51, 53]:

$$[DNA]/(\varepsilon_a-\varepsilon_f) = [DNA]/(\varepsilon_b-\varepsilon_f) + 1/K_b(\varepsilon_a-\varepsilon_f),$$

where $\varepsilon_a = A_{obsd}/[complex]$, ε_a = extinction coefficient for the free complex, and ε_b = extinction coefficient for the complexes in the fully bound form. The high value of K_b obtained for $[Zn(PEF)Cl(H_2O)]$, $[Pt(PEF)Cl(H_2O)]\cdot 3H_2O$, $[Fe(PEF)Cl_2(H_2O)_2]\cdot 5H_2O$, and $[Ru(PEF)Cl_2(H_2O)_2]\cdot 5H_2O$ suggest a strong binding of complexes to CT-DNA (table 4). Indeed, it is much higher than K_b calculated for pefloxacin ($=1\pm 0.03\times 10^3\ (mol\,L^{-1})^{-1}$), indicating that the coordination of pefloxacin ligand to M(II)/(III) ion significantly enhances the ability to bind to CT-DNA. K_b of $[Cu(PEF)_2]\cdot 4H_2O$, $[Zn(PEF)Cl(H_2O)]$, $[Pt(PEF)Cl(H_2O)]\cdot 3H_2O$, $[Fe(PEF)Cl_2(H_2O)_2]\cdot 5H_2O$, and $[Ru(PEF)Cl_2(H_2O)_2]\cdot 5H_2O$ are higher than the EB-binding affinity for

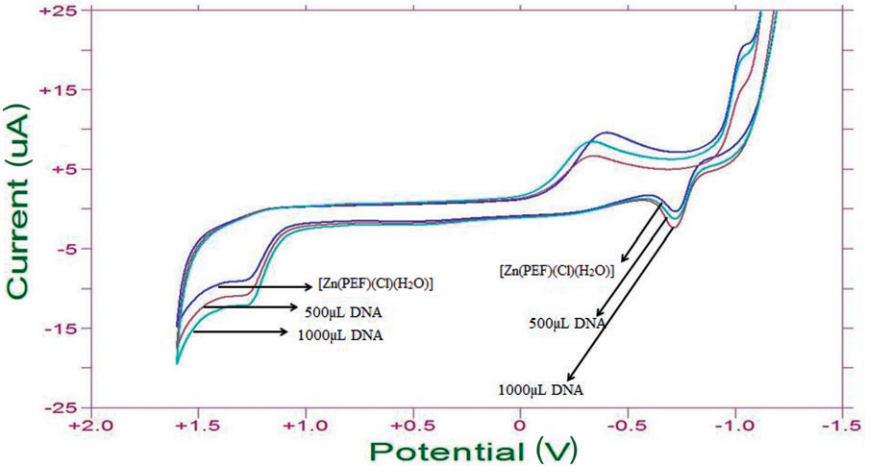

Figure 2. Cyclic voltammograms in the range −1.5 to +2 V of 1×10^{-4} mol L^{-1} [Zn(PEF)Cl(H_2O)] in Tris-HCl buffer solution in the absence or presence of CT scan rate = 100 mV s^{-1}.

DNA ($K_b = 1.23 \pm 0.07 \times 10^5$), suggesting that electrostatic and intercalative interactions may affect EB displacement [20, 40, 41, 50]. The K_b values are given in table 4.

The electrochemical investigations of metal–DNA interactions provide a useful complement to spectroscopic methods and yield information about interactions with both the reduced and oxidized form of the complex [20, 40, 41, 50]. In Supplementary material and figure 2, the cyclic voltammograms of [Zn(PEF)Cl(H_2O)] in the absence and presence of CT-DNA with diverse r values in Tris-HCl (pH 7) buffer solution are shown. Electrochemical potential of a small molecule will shift positively when it intercalates into DNA double helix, but if bound to DNA by electrostatic interaction, would shift in a negative direction [20, 40, 41, 50]. In the case of more potentials than one, a positive shift of E_{p1} and a negative shift of E_{p2} imply that the molecule can bind to DNA by both intercalation and electrostatic interaction [20, 54]. The quasi-reversible redox couple for each complex in 1/9 methanol/buffer solution has been studied upon addition of CT-DNA; shifts of the cathodic E_{pc} and anodic E_{pa} potentials are given in table 5. No new redox peaks appeared after the addition of CT-DNA to each complex, but the current intensity of all the peaks increased significantly, suggesting interaction between each complex and CT-DNA. The increase in current intensity can be explained as an equilibrium mixture of free and DNA-bound complex to the electrode surface [40]. [Zn(PEF)Cl(H_2O)] exhibits the same electrochemical behavior upon addition of CT-DNA at diverse r values. For increasing amounts of CT-DNA, the anodic potential E_{pa1} did not change after DNA-binding but the cathodic potential E_{pc} shows a positive shift ($\Delta E_{pc} = +402$ mV for [Zn(PEF)Cl(H_2O)], while the anodic potential E_{pa2} shifts to more negative values ($\Delta E_{pa} = -55$ mV)). These shifts of potentials show the complexes bind to DNA by both intercalation and electrostatic interaction [54]. A positive shift of the cathodic potential (($\Delta E_{pc} = +402$ mV) of [Zn(PEF)Cl(H_2O)] is observed while the first anodic potential remains unchanged (figure 2) followed by a slight increase in current intensity, suggesting intercalation between [Zn(PEF)Cl(H_2O)] and CT-DNA [40, 41]. The conclusion derived from the CV study is that the complexes bind to DNA

Table 5. Cathodic and anodic potentials and the shift of the potentials in the absence and presence of CT-DNA of [Zn(PEF)Cl(H_2O)].

Complex	Redox couple	$E_pa_1^f$	$E_pc_1^f$	ΔE_1^f	$(E_{1/2}^f)_1$	$E_pa_2^f$	$E_pa_2^f$	ΔE_2^f	$(E_{1/2}^f)_2$
[Zn(PEF)Cl(H_2O)]	Zn/Zn(II)	−726	−1030	304	152	1258	−379	1637	818.5
Complex	$E_pa_1^b$	$E_pa_2^b$	ΔE_1^b	$(E_{1/2}^b)_1$	$E_pa_2^b$	$E_pc_2^b$	ΔE_2^f	$(E_{1/2}^f)_2$	
[Zn(PEF)Cl(H_2O)]	−725	−1026	301	150.5	1282	−324	1606	803	

Table 6. Antimicrobial and antifungal activity of PEF and metal complexes.

Compound	1	2	3	4	5	6	7	8	9
PEF	12	12	12	14	13	14	22	24	12
[Fe(PEF)Cl_2(H_2O)$_2$]·5H_2O	34	26	36	40	33	40	28	36	38
[Pt(PEF)Cl(H_2O)]·3H_2O	36	28	38	38	35	42	32	36	40
[Cu(PEF)$_2$]·4H_2O	34	25	38	35	30	35	24	30	38
[Ru(PEF)Cl_2(H_2O)$_2$]·5H_2O	35	26	34	34	28	34	26	28	36
[Zn(PEF)Cl(H_2O)]	36	28	35	36	32	36	30	30	40

1: *C. albicans*, 2: *S. cerevisiae*, 3: *E. coli*, 4: *E. cloacae*, 5: *B. megaterium*, 6: *B. cereus*, 7: *Pseudomonas* sp., 8: *B. melitensis*, 9: *S. aureus* (amount absorbed by the bacteria 500 μg).

by both intercalation and electrostatic interaction. $E_{1/2}$ values of all complexes decrease after DNA addition.

3.4. *Antibacterial and antifungal activities*

The susceptibility of certain strains of bacteria toward PEF and its complexes was judged by measuring the size of inhibition zone diameter. Antibacterial activities of PEF and its complexes have been carried out with three Gram-positive (*B. megaterium*, *B. cereus*, *S. aureus*) and four Gram-negative (*E. coli*, *E. cloacae*, *Pseudomonas* sp., *B. melitensis*) bacteria. Antifungal screenings were tested against two fungi (*C. albicans*, *S. cerevisiae*). The results are summarized in table 6. The compounds have remarkable bactericidal and fungicidal properties. All the complexes show excellent activity against all types of bacteria and fungi.

4. Conclusion

Pefloxacin complexes with Cu(II), Pt(II), Zn(II), Fe(III), and Ru(III) have been synthesized and characterized by physicochemical and spectroscopic methods. Pefloxacin is deprotonated and bidentate, bound to the metal through pyridine oxygen and one carboxylate oxygen. In the cyclic voltammograms of the complexes recorded in acetonitrile/water (1/1, v/v) solution quasi-reversible waves attributed to redox couples, characteristic for each metal complex, have been recorded at expected potentials. The study of complex interaction with CT-DNA has been performed with UV spectroscopy and CV, revealing that the complexes bind DNA.

$[Pt(PEF)Cl(H_2O)]\cdot 3H_2O$ exhibits much higher intrinsic binding constant to CT-DNA than the other complexes. The results show that changing the metal environment can modulate the binding of the complex with DNA [42]. DNA adducts of $[Pt(PEF)Cl(H_2O)]\cdot 3H_2O$ could lead to a broader spectrum of antibacterial activity. Cyclic voltammetric studies show that all complexes bind to CT-DNA by both intercalation and electrostatic interaction. Antibacterial properties of pefloxacin complexes with different metal ions tested for activity against diverse microorganisms show antimicrobial activity comparable to free fluoroquinolones. In certain examples the activities were increased, for example, norfloxacin complexes with zinc, iron, and silver; the magnesium complex with ciprofloxacin is characterized by a slight decrease in antibacterial activity. Vanadium–ciprofloxacin complex is promising with respect to its insulin–mimetic behavior and its concomitant low toxicity in the physiological concentration range [42]. According to our biological results, all complexes exhibited higher inhibitory activity than pefloxacin.

Acknowledgments

The authors thank TUBITAK (Project No: 109T020) and KSU (Project No: 2009/2-8) for financial support.

References

[1] J.S. Wolfson, D.C. Hooper. *Clin. Microbiol. Rev.*, **2**, 378 (1989).
[2] E.M. Scholar. *Am. J. Pharm. Educ.*, **66**, 164 (2002).
[3] L.A. Mitscher. *Chem. Rev.*, **105**, 559 (2005).
[4] V.T. Andriole (Ed.). *The Quinolones*, 3rd Edn, Academic Press, San Diego (2000).
[5] N. Sultana, M.S. Arayne, S. Gul, S. Shamim. *J. Mol. Struct.*, **975**, 285 (2010).
[6] B. Lippert. *Coord. Chem. Rev.*, **200**, 487 (2000).
[7] M. Gellert, K. Mizuuchi, M.H. O'Dea, H.A. Nash. *Proc. Natl Acad. Sci. USA*, **73**, 3872 (1976).
[8] S. Sagdinc, S. Bayari. *J. Mol. Struct.*, **691**, 107 (2004).
[9] H.R. Park. *Bull. Korean Chem. Soc.*, **21**, 849 (2000).
[10] A. Serafin, A. Stanczak. *Russ. J. Coordin. Chem.*, **35**, 81 (2009).
[11] M.N. Patel, P.A. Parmar, D.S. Gandhi. *J. Enzyme Inhibit. Med., Chem.*, **26**, 188 (2011).
[12] A.R. Shaikh, R. Giridhar, F. Megraud. *Acta Pharm.*, **59**, 259 (2009).
[13] H.W. Sun, P.Y. Chen, F. Wang. *Talanta*, **79**, 134 (2009).
[14] G.Z. Li, Y.M. Liu, G.Z. Li. *Spectrosc. Spectr. Anal.*, **24**, 1086 (2004).
[15] S. Lecomte, M.H. Baron. *Biospectroscopy*, **3**, 31 (1997).
[16] S. Lecomte, M.T. Chenon. *Int. J. Pharm.*, **139**, 105 (2009).
[17] S. Lecomte, M.H. Baron, M.T. Chenon, C. Coupry, N.J. Moreau. *Antimicrob. Agents Chemotherapy*, **38**, 2810 (1994).
[18] M.J. Clarke. *Coord. Chem. Rev.*, **236**, 209 (2003).
[19] P.T. Selvi, H. Stoeckli-Evans, M. Palaniandavar. *J. Inorg. Biochem.*, **99**, 2110 (2003).
[20] G. Psomas. *J. Inorg. Biochem.*, **102**, 1798 (2008).
[21] L. Messori, J. Shaw, M. Camalli, P. Mura, G. Marcon. *Inorg. Chem.*, **42**, 6166 (2003).
[22] K.E. Erkkila, D.T. Odom, J.K. Barton. *Chem. Rev.*, **99**, 2777 (1999).
[23] D.R. Xiao, E.B. Wang, H.Y. An, Z.M. Su, Y.G. Li, L. Gao, C.Y. Sun, L. Xu. *Chem. A Eur. J.*, **11**, 6673 (2005).
[24] E.L. Hegg, J.N. Burstyn. *Coord. Chem. Rev.*, **173**, 133 (1998).
[25] M. Gonzalez-Alvarez, G. Alzuet, B. Borras, B. Macias. *Inorg. Chem.*, **42**, 2992 (2003).
[26] D.S. Sigman, A. Mazumder, D.M. Perin. *Chem. Nucleases Chem. Rev.*, **93**, 2295 (1993).

[27] V. Rajendiran, R. Karthik, M. Palaniandavar, H. Stoeckli-Evans, V.S. Periasamy, M.A. Akbarsha, B.S. Sriang, H. Krishnamurty. *Inorg. Chem.*, **46**, 8208 (2007).
[28] N. Raman, R. Jeyamurugan. *J. Coord. Chem.*, **62**, 2375 (2009).
[29] Y.L. Song, Y.T. Li, Z.Y. Wu. *J. Inorg. Biochem.*, **102**, 1691 (2008).
[30] Y.Y. Kou, J.L. Tian, D.D. Li, H. Liu, W. Gu, S.P. Yan. *J. Coord. Chem.*, **62**, 2182 (2009).
[31] F. Jelen, M. Tomschik, P. Emil. *J. Electroanal. Chem.*, **423**, 141 (1997).
[32] F. Jelen, M. Tomschik, P. Emil. *J. Electroanal. Chem.*, **427**, 49 (1997).
[33] A. Erdem, O.A. Dilsat, K. Hakan, K. Pinar, S. Aylin, S. Arzu, O. Mehmet. *Electrochem. Commun.*, **7**, 815 (2005).
[34] Y. Yardim, E. Keskin, A. Levent, M. Ozsoz, Z. Senturk. *Talanta*, **80**, 1347 (2010).
[35] A. Golcu, D.B. Topal, S.A. Ozkan. *Anal. Lett.*, **38**, 1913 (2005).
[36] J.M. Kauffmann, J.C. Vire. *Anal. Chim. Acta*, **273**, 329 (1993).
[37] J. Marmur. *J. Mol. Biol.*, **3**, 208 (1961).
[38] J. Marmur, R.D. Hotchkiss. *Lab. Pathol. Microbiol.*, **40**, 55 (1954).
[39] M. Carter, A.J. Bard, M. Rodriguez. *J. Am. Chem. Soc.*, **111**, 8901 (1989).
[40] E.K. Efthimiadou, A. Karaliota, G. Psomas. *Inorg. Chim. Acta.*, **360**, 4093 (2007).
[41] A. Tarushi, E.K. Efthimiadou, P. Christofis, G. Psomas. *Inorg Chim. Acta*, **360**, 3978 (2007).
[42] I. Turel, A. Golobic, A. Klavzar, B. Pihlar, P. Buglyo, E. Tolis, D. Rehter, K. Sepcic. *J. Inorg. Biochem.*, **95**, 199 (2003).
[43] S.E. Castillo-Blum, N. Barba-Behrens. *Coord. Chem. Rev.*, **196**, 3 (2000).
[44] A.H. El-Masry, H.H. Fahmy, S.H.A. Abdelwahed. *Molecules*, **5**, 1429 (2000).
[45] A. Golcu, M. Tumer, H. Demirelli. *Inorg. Chim. Acta*, **358**, 1785 (2005).
[46] A.M. Beltagi. *J. Pharm. Biomed. Anal.*, **31**, 1079 (2003).
[47] B. Uslu, B.D. Topal, S.A. Ozkan. *Talanta*, **74**, 1191 (2008).
[48] S.A. Ozkan, B. Uslu, H.Y. Aboul-Enein. *Talanta*, **61**, 147 (2003).
[49] S.A. Ozkan, B. Uslu, P. Zuman. *Anal. Chim. Acta*, **501**, 227 (2004).
[50] V. Tangoulis, G. Psomas, C.S. Dendrinou, C.P. Raptopoulou, A. Terzis, D.P. Kessissoglou. *Inorg. Chem.*, **35**, 7655 (1996).
[51] E.C. Long, J.K. Barton. *Acc. Chem. Res.*, **23**, 271 (1990).
[52] J.M. Kelly, A.B. Tossi, D.J. McConnell, C. Uigin. *Nucl. Acids Res.*, **17**, 6017 (1985).
[53] A.M. Pyle, J.P. Rehmann, R. Meshoyrer, C.V. Kumar, N.J. Turro, K.B. Jacqueline. *J. Am. Chem. Soc.*, **111**, 3051 (1989).
[54] K. Jiao, Q.X. Wang, W. Sun, F.F. Jian. *J. Inorg. Biochem.*, **99**, 1369 (2005).